

Vitamin D Attenuates Endothelial Dysfunction in Uremic Rats and Maintains Human Endothelial Stability

Marc Vila Cuenca, MSc; Evelina Ferrantelli, PhD; Elisa Meinster, MSc; Stephan M. Pouw, MSc; Igor Kovačević, PhD; Renné X. de Menezes, PhD; Hans W. Niessen, PhD; Robert H.J. Beelen, PhD; Peter L. Hordijk, PhD; Marc G. Vervloet, MD, PhD

Background—Dysfunctional endothelium may contribute to the development of cardiovascular complications in chronic kidney disease (CKD). Supplementation with active vitamin D has been proposed to have vasoprotective potential in CKD, not only by direct effects on the endothelium but also by an increment of α -Klotho. Here, we explored the capacity of the active vitamin D analogue paricalcitol to protect against uremia-induced endothelial damage and the extent to which this was dependent on increased α -Klotho concentrations.

Methods and Results—In a combined rat model of CKD with vitamin D deficiency, renal failure induced vascular permeability and endothelial-gap formation in thoracic aorta irrespective of baseline vitamin D, and this was attenuated by paricalcitol. Downregulation of renal and serum α -Klotho was found in the CKD model, which was not restored by paricalcitol. By measuring the real-time changes of the human endothelial barrier function, we found that paricalcitol effectively improved the recovery of endothelial integrity following the addition of the pro-permeability factor thrombin and the induction of a wound. Furthermore, immunofluorescence staining revealed that paricalcitol promoted vascular endothelial-cadherin–based cell-cell junctions and diminished F-actin stress fiber organization, preventing the formation of endothelial intracellular gaps.

Conclusions—Our results demonstrate that paricalcitol attenuates the CKD-induced endothelial damage in the thoracic aorta and directly mediates endothelial stability in vitro by enforcing cell-cell interactions. (*J Am Heart Assoc.* 2018;7:e008776. DOI: 10.1161/JAHA.118.008776)

Key Words: chronic kidney disease • endothelial dysfunction • Klotho • vitamin D

The risk of cardiovascular-related mortality is exceedingly high in individuals with chronic kidney disease (CKD).¹ Impairment of endothelial function, which accompanies CKD,² is recognized as a sentinel event in the development and progression of cardiovascular disease.³ As kidney function declines, there is a progressive decline of both plasma 25 hydroxyvitamin D (25(OH)D) and 1,25-dihydroxyvitamin D (1,25(OH)₂D) concentrations, and of the kidney-derived protein α -Klotho, accompanied by secondary hyperparathyroidism and increased fibroblast growth factor-23 levels.^{4,5} These hormonal disturbances occur already in early-stage CKD and are proposed to make a notable contribution to the initiation and progression of cardiovascular disease.^{6,7} Remarkably, there is limited

evidence directly pointing to structural abnormalities and a mechanistic role for the endothelial layer in CKD.

Treatment with active vitamin D has been considered a key therapy for cardiovascular events in CKD,⁸ but controversy remains as beneficial effects on cardiac abnormalities as observed in animal models⁹ could not be confirmed in clinical trials.^{10,11} Moreover, while in vitro studies suggested a protective role for vitamin D in ameliorating damaged endothelium,^{12,13} experimental in vivo CKD studies have primarily focused on the prevention of vascular calcification of the medial layer and heart failure^{9,14,15} but paid little attention to structural endothelial damage. A small number of prior studies have suggested benefits of the active vitamin D analogue

From the Departments of Nephrology (M.V.C., M.G.V.), Molecular Cell Biology and Immunology (E.F., S.M.P., R.H.J.B.), Pathology and Cardiac Surgery (E.M., H.W.N.), Physiology (I.K., P.L.H.), and Epidemiology and Biostatistics (R.X.d.M.), VU University Medical Center, Amsterdam, The Netherlands; Amsterdam Cardiovascular Sciences, Amsterdam, The Netherlands (M.V.C., I.K., H.W.N., P.L.H., M.G.V.).

Accompanying Figures S1 and S2 are available at <https://www.ahajournals.org/doi/suppl/10.1161/JAHA.118.008776>

Correspondence to: Marc Vervloet, MD, PhD, Department of Nephrology, VU University Medical Center, 1007 MB Amsterdam, The Netherlands. E-mail: m.vervloet@vumc.nl

Received February 17, 2018; accepted July 9, 2018.

© 2018 The Authors. Published on behalf of the American Heart Association, Inc., by Wiley. This is an open access article under the terms of the Creative Commons Attribution-NonCommercial License, which permits use, distribution and reproduction in any medium, provided the original work is properly cited and is not used for commercial purposes.

Clinical Perspective

What Is New?

- Besides established effects on calcification and vasomotor function, this study shows that uremia induces endothelial barrier dysfunction.
- Supplementation with active vitamin D attenuated this uremia-mediated endothelial permeability and barrier disruption.
- This study also reveals underlying mechanisms, which include enforced endothelial cell-cell connections by active vitamin D.

What Are the Clinical Implications?

- These findings should raise awareness of additional vasculotoxic effects of uremia, including loss of endothelial barrier integrity.
- This study reveals that active vitamin D may be an effective therapeutic strategy for endothelial dysfunction in chronic kidney disease, and our results may serve as a warning signal for current reluctance to the use of active vitamin D, as reflected by clinical practice guidelines.
- The endothelial protective effects from active vitamin D against an injury and increased permeability may be of interest for other vascular-related diseases.

paricalcitol on endothelial stability in animal models of CKD^{16,17} and even in patients.^{18,19} Interestingly, paricalcitol supplementation increased kidney and serum α -Klotho levels in in vivo models of CKD.^{20,21} α -Klotho is an antiaging protein, and its deficiency is associated with a cardiovascular phenotype including arteriosclerosis, vascular calcification, and, importantly, endothelial cell dysfunction.^{22,23} In humans, deficiency in serum α -Klotho correlates with cardiovascular complications.²⁴ However, a direct role of serum α -Klotho deficiency on endothelial dysfunction in patients with CKD has not been established.

In the present study, we evaluated the impact of vitamin D deficiency and α -Klotho concentrations and the effect of paricalcitol treatment on the development of endothelial cell dysfunction in a CKD rat model. Our data show that paricalcitol treatment attenuates endothelial damage in CKD and directly mediates endothelial stability in vitro. This beneficial effect was not mediated by an increment of α -Klotho concentrations, identifying paricalcitol as a key intervention stabilizing endothelial barrier function.

Methods

The data, analytic methods, and study material will not be made available to other researchers for the purpose of reproducing the results or replicating the procedure.

Experimental Models

Male Wistar rats (Charles River, Maastricht, The Netherlands) weighing 250 to 275 g were used. After 1 week of acclimatization, 3/4 nephrectomy was performed to induce uremia (CKD); healthy (non-CKD) controls were not surgically manipulated (experimental design on Figure 1A). The 3/4 nephrectomy involved the complete removal of the right kidney and ligation of 1 to 2 branches of the arteries supplying the left kidney in order to obtain residual kidney function of about one fourth of the total capacity. Animals were anesthetized with inhaled isoflurane (2%). For analgesia, tamgesic was administered (10 μ L/g weight) intramuscularly pre- and postoperatively. Thirty-two rats were made uremic by 3/4 nephrectomy. Four of the rats died during the surgery (n=28). Following 1 week of recovery from the 3/4 nephrectomy (week 1), animals were fed a vitamin D-deficient diet (Diet code: TD.120503 Vitamin D deficient diet; 20% lactose, 1% Ca, 0.65% P) and it was maintained until the end of the experiment as we described recently.²⁵ To induce CYP24A1 expression, to accelerate the catabolism of endogenous 25(OH)D and calcitriol stores, the rats were subcutaneously injected with 32 ng of paricalcitol (Zemplar[®], kindly provided by AbbVie) 3 times per week for 3 weeks in total. Non-vitamin D-deficient groups received a standard diet (Teklad Global 2016, Envigo). Oral administration of paricalcitol (0.1 μ g/kg rat; kindly provided by AbbVie, Chicago) dissolved in sugar water (1%) was provided 3 times per week for 7 weeks in total. In parallel, vehicle control rats received only sugar water (1%). Food consumption was measured every day. All the animals were socially housed under standard conditions and were given food and water ad libitum. Health conditions were checked daily. The weight of the animals was checked daily after surgery for 7 days and weekly for the remainder of the experiment. Animals that lost more than 20% of their maximum gained body weight at any point during the experiment or showed abnormal activity were excluded from the experiment. Animals were organized as indicated in Figure 1A: non-CKD group standard diet with vehicle control treatment (n=6), paricalcitol treatment (n=6), non-CKD group with vitamin D deficient diet with vehicle control treatment (n=6), paricalcitol treatment (n=6), CKD group standard diet with vehicle control treatment (n=7), paricalcitol treatment (n=7), CKD group vitamin D-deficient diet with vehicle control treatment (n=8), paricalcitol treatment (n=6). At the end of the experiment, euthanasia was performed using CO₂/O₂ asphyxiation. The experimental protocol was in compliance with the National Institutes of Health's Guide for the Care and Use of Laboratory Animals and was approved by the Animal Welfare Committee at the VU University Medical Center, Amsterdam.

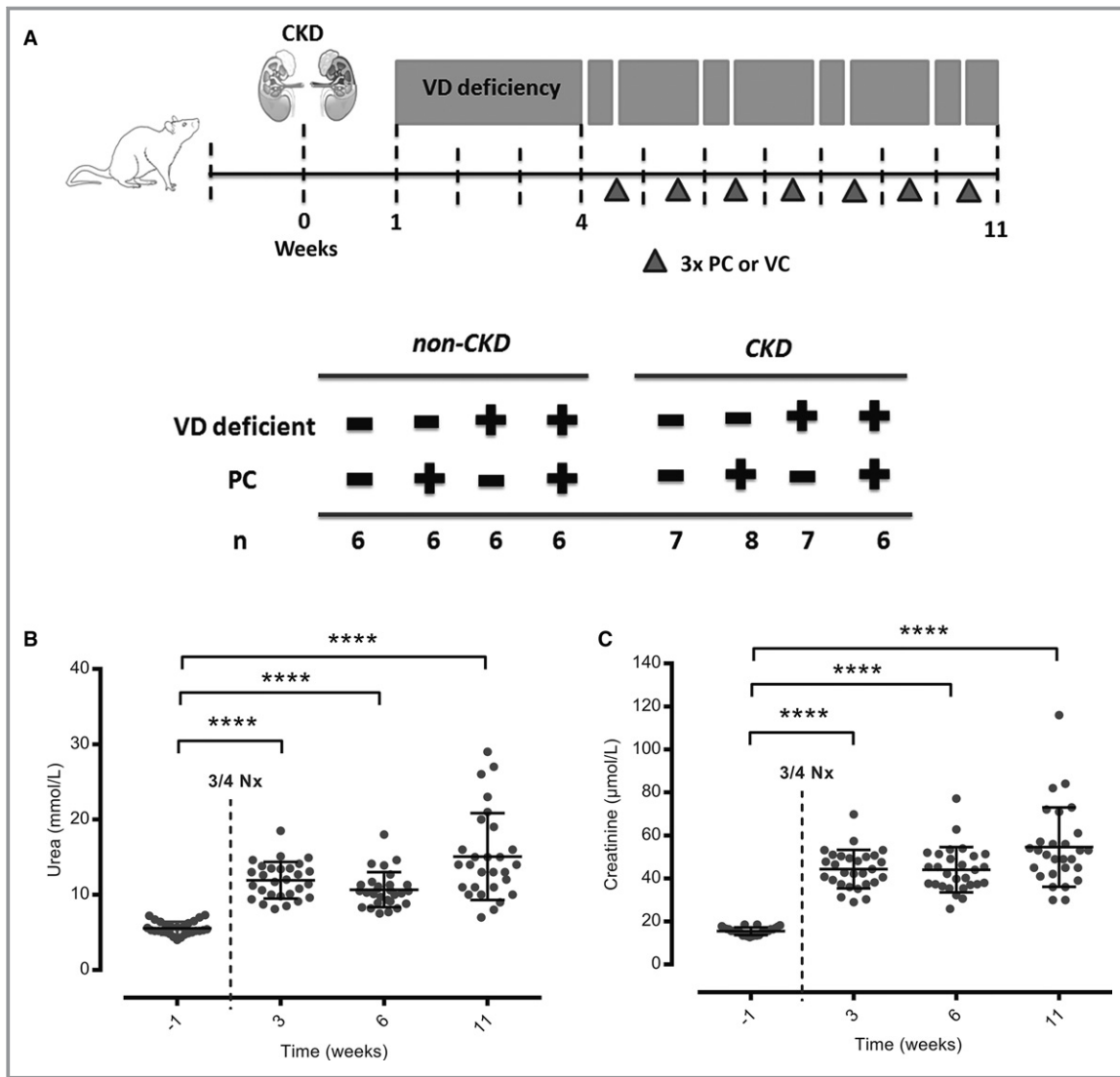


Figure 1. Uremia and vitamin D deficiency is established. A, Representative experimental design and group distribution. CKD was induced by 3/4 nephrectomy (3/4 Nx) at week 0. Vitamin D deficiency was induced from week 1 to week 4 and vitamin D–deficient diet was maintained until the end of the experiment (week 11). Concurrently, animals received oral paricalcitol (0.1 µg/kg) or vehicle control treatment 3 times per week for 7 weeks in total. Bottom, An overview of the groups. (CKD indicates uremic animals; non-CKD, nonuremic animals; PC, paricalcitol; VC, and VD, vitamin D). Scatter plot analyses of serum levels of urea (mmol/L) (B) and creatinine (µmol/L) (C) before (week –1) and after (weeks 3, 6, and 11) surgery. Results are means±SD (n=28). Differences were considered statistically significant for $P<0.05$, using 1-way (repeated measures) ANOVA. (3/4 Nx=induction of 3/4 nephrectomy) **** $P<0.0001$. Serum levels of (D) inactive (25(OH)D; nmol/L) and (E) active (1,25(OH)₂D; pmol/L) forms of vitamin D 3 weeks after vitamin D deficiency (week 4). Results are means±SD (n=12–15). #Indicates that most of the values were under the detection level and significance could not be calculated for that group. (CKD indicates uremic animals; non-CKD, nonuremic animals; and VD, vitamin D). Differences were considered statistically significant for $P<0.05$, using 2-way ANOVA in D ($P=0.0064$ for surgery, $P<0.0001$ for diet, $P=0.0545$ for surgery×diet) and unpaired t test for E. ** $P<0.001$.

Measurement of Blood Parameters

Five hundred microliters of blood were drawn from the tail vein in rats under inhaled isoflurane (2%) anesthesia. At weeks –1, 3, 6, and 10, serum samples from CKD groups were analyzed for urea and creatinine levels. For determination of urea levels, a kinetic test with urease and glutamate dehydrogenase was

used. Creatinine levels were detected by indirect immunofluorescence assay. Measurements were performed by using spectrophotometer Cobas8000 C702 (Roche Diagnostics, Risch-Rotkreuz, Switzerland). At week 4, serum samples were analyzed for 25(OH)D by competitive binding protein assay (Diasorin, Stillwater, Minnesota) and 1,25(OH)₂D by radioimmunoassay after immunoextraction (IDS, Tyne and Wear, UK).

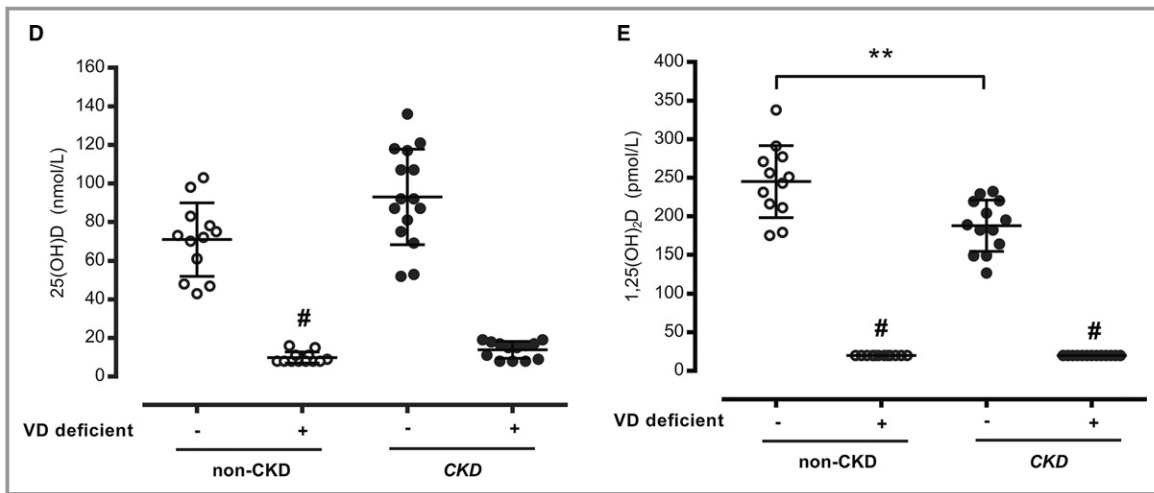


Figure 1. (Continued)

Parathyroid hormone (PTH) serum levels from the end point (week 11) were analyzed by ELISA (Scantibodies Laboratory, Santee, CA) as previously described.²⁵

Evans Blue Extravasation in the Thoracic Aorta

Vascular permeability was assessed by injecting 4% of Evans Blue dye (Sigma) in 0.9% of saline via the tail vein (1 mL/kg) under isoflurane (2%) anesthesia. After 30 minutes of Evans Blue dye injection, animals were euthanized for tissue harvest. The thoracic aorta was removed, weighed after washing with phosphate-buffered saline (PBS), and the dye was extracted in formamide at 56°C for 24 hours. Dye concentration was quantified from the light absorbance at 620 nm, and its tissue content was calculated from a standard curve of dye concentration in the range of 0.5 to 10 µg/mL. The Evans Blue concentration in tissue was corrected by the weight of tissue and Evans Blue concentration in plasma (ng/mL dye in tissue/mg tissue/ng per milliliter dye in plasma).

Histology and Immunohistochemistry

For immunohistochemical analysis, 4-µm sections were deparaffinized, rehydrated, and incubated in methanol/H₂O₂ (0.3%) for 30 minutes to block endogenous peroxidases. Antigen retrieval was performed with boiling 0.01 mol/L citrate buffer (pH 6.0). Tissue slides were then preincubated with normal rabbit serum (1:50, Dako, Eindhoven, The Netherlands) for 10 minutes at room temperature. Next, slides were incubated overnight at 4°C with goat-antirat PECAM-1 (CD31, clone M-20; 1:50, Santa Cruz Biotechnology, CA) and then incubated with rabbit-antigoat-horseradish peroxidase (1:100, Dako) for 30 minutes at room temperature. Staining was visualized using 3,3'-diaminobenzidine (0.1 mg/mL, 0.02% H₂O₂). The slides were subsequently counterstained with hematoxylin,

dehydrated, and covered. Stainings of phosphate-buffered saline controls were included. These controls yielded negative results (data not shown). The sections were scanned using the Panoramic Desk scanner (3DHitech, Budapest, Hungary). Analyses were assessed with Pannoramic Viewer (3DHitech, Budapest, Hungary), endothelial gaps were determined by measuring Negative CD31 surface *100/µm total CD31 from 3 random areas of the aortic tissue.

Quantitative Reverse Transcription Polymerase Chain Reaction

Kidney tissues were mechanically homogenized and total RNA was extracted using TRIzol Reagent (Invitrogen). Reverse transcription into cDNA was performed using the Reverse Transcription System kit (Promega, Madison, WI). The synthesized cDNA was amplified with a standard quantitative polymerase chain reaction (qPCR) protocol including the use of SYBER GREEN (Applied Biosystems). *Klotho* forward: GAGCGGTCACCTAAGCGAATACG reverse: CGTGAATGAGGTCT-GAAAGC; *β-actin*, forward: GACCAGAGGCATACAGGGACAA, reverse: GGCCAACCGTGAAAAGATGA. The relative amount of mRNA was calculated using comparative Ct (ΔΔCt) methods. Amplification products were normalized against *β-actin* mRNA, which was amplified in the same reaction as an internal control. The fold change in mRNA expression was quantified relative to control (healthy nontreated) animals.

α-Klotho Immunoblot

Kidney lysates were prepared by homogenizing preserved tissue in lysis buffer containing Protease Inhibitor Cocktail (Roche Applied Science, Indianapolis, IN). Protein concentrations were determined using the Pierce Micro BCA Protein Assay Kit (Thermo Scientific, Rockford, IL), and 20 µg of protein was used

for α -Klotho immunoblot with the following antibodies: rat antihuman Klotho monoclonal antibody (KM2076 at 1:1000 dilution, Transgenic Inc, Kobe, Japan), GAPDH (14C10 at 1:1000 Cell Signalling, Leiden, The Netherlands), followed by donkey antirat/rabbit conjugated with horseradish peroxidase (1:5000, Dako). Signal was visualized using enhanced chemiluminescence (Life Sciences) on LAS3000 (Fujifilm, Japan). Image J (NIH, Bethesda, Maryland) was used for analysis. For the immunoprecipitation-immunoblotting, α -Klotho assay in serum from the end point (week 11) was performed as previously described.²⁶

Human Endothelial Cell Culture

Human umbilical vein endothelial cells (HUVECs) were isolated from umbilical cords from healthy donors obtained from the Amstelland Ziekenhuis, Amstelveen. The use of human tissue for isolation of endothelial cells was approved by the Medical Ethical Committee of the VU University Medical Center. Patients gave informed consent for the use of tissue for research purposes. The study conforms with the Declaration of Helsinki. After isolation, cells were resuspended in M199 medium (Biowhittaker/Lonza), supplemented with penicillin 100 U/mL and streptomycin 100 μ g/mL (Biowhittaker/Lonza), heat-inactivated human serum 10% (Sanquin Blood Supply, Amsterdam, The Netherlands), heat-inactivated newborn calf serum 10% (Gibco, Grand Island, NY), crude endothelial cell growth factor 150 μ g/mL (prepared from bovine brains), L-glutamine 2 mmol/L (Biowhittaker/Lonza), and heparin 5 U/mL (Leo Pharmaceutical Products, Weesp, The Netherlands). Cells were cultured at 37 °C and 5% CO₂, with a change of culture medium every 2 days. Cells were cultured up to passage 2; for experiments, passage 1 to 2 cells were used.

Endothelial Barrier Function Assay

For electric cell-substrate impedance sensing measurements, cells were seeded in 1:1 density on L-cysteine (10 mmol/L, Sigma) and gelatin-coated electric cell-substrate impedance sensing arrays, each containing 8 wells with 10 gold electrodes per well in a 0.49 mm² electrode area (Applied Biophysics, Troy, NY)²⁷. Electric cell-substrate impedance sensing software (v1.2.65.0 PC; Applied BioPhysics) was used to calculate the level of overall resistance (at 4000 Hz). Culture medium was renewed 24 hours after seeding, and experiments were performed 48 hours after seeding. For stimulation, pretreatment medium was changed for 1% human serum albumin (Sanquin Blood Supply) in M199 medium containing recombinant human Klotho from Sigma (400 pM) and paricalcitol (10–100 nmol/L; kindly provided by AbbVie, Chicago, IL). After 24 hours of pretreatment, thrombin (1 U/mL; Sigma Aldrich, Zwijndrecht, The Netherlands) was added directly to the wells for a final concentration of 1 U/mL or

electrical wounding was applied (60 s; 100 000 Hz), respectively. Thrombin was quantified by the percentage of drop in resistance after the addition of thrombin, and the area under the curve was quantified from normalized baseline starting from time 0 hour. Wound healing quantification was assessed by the slope of the wound healing (1–3 hours) and the area under the curve measured starting from 1 hour.

Immunofluorescence Imaging

HUVECs were seeded on glass coverslips coated with glutaraldehyde 0.5% (Fluka, St. Gallen, Switzerland) cross-linked gelatine. Cells were seeded at 1:1 density and grown to confluence in 24 to 48 hours. Pretreatment was performed in 1% human serum albumin in M199, containing Klotho (400 pmol/L) or paricalcitol (10–100 nmol/L). After 24 hours of pretreatment, thrombin was added to the wells, for a final concentration of 1 U/mL. At indicated time points (0, 60, and 120 minutes), the medium was replaced by 2% paraformaldehyde (37°C, Sigma Aldrich), followed by 15 minutes of incubation on ice. Cells were permeabilized with Triton X-100 0.05% (Sigma Aldrich) in phosphate-buffered saline and incubated overnight with primary antibody against vascular endothelial (VE)-cadherin (1:400; XP D87F2, Cell Signaling). Subsequently, cells were washed and incubated with fluorescein isothiocyanate-conjugated secondary antibodies (1:100; Invitrogen, Paisley, United Kingdom), and the F-actin cytoskeleton was visualized with rhodamine/phalloidin (1:140; PHDH1 Cytoskeleton Inc, Denver, CO) for 2 hours at room temperature. Cells were washed and nuclei were stained with 4',6-diamidino-2-phenylindole (1:500; Sigma Aldrich) for 15 minutes. Next, cells were washed, and sealed with Mowiol mounting medium (Sigma Aldrich). Imaging was performed with a Leica TCS SP8 STED using a 63 \times Zeiss oil objective. Image J (National Institutes of Health, Bethesda, MD) was used for analysis. For quantification of VE-cadherin/F-actin, images were equally adjusted for contrast and mean fluorescence was quantified and divided by the number of counted nuclei (4',6-diamidino-2-phenylindole).

Statistical Analysis

Data were analyzed using both GraphPad Prism 7 software (La Jolla, CA) and the statistical package R (version 3.4.3)²⁸. Two-group comparisons were made by paired or unpaired t tests. ANOVA (involving a single, 2, or 3 factors) was also used to perform comparisons, with Bonferroni multiple-testing correction applied where appropriate, as indicated in figure legends. Analysis of the different factors and their 2-way and 3-way interactions are reported in Table. Correlation was assessed by using Pearson correlation. Differences were considered statistically significant for $P < 0.05$.

Table. Analysis of the Different Independent Variables and Their Interactions for Each Dependent Variable

Independent Variables	Dependent Variables								
	25(OH)D	Leakage	CD31	Protein α-Klotho	mRNA α-Klotho	Soluble α-Klotho	Creatinine	Urea	PTH
	Pr(>F)	Pr(>F)	Pr(>F)	Pr(>F)	Pr(>F)	Pr(>F)	Pr(>F)	Pr(>F)	Pr(>F)
Surgery	0.0064*	0.003*	<2 ⁻¹⁶ *	<2 ⁻¹⁶ *	0.001*	0.001*	0.003*
Treatment	-	0.021*	0.041*	0.935	0.881	0.051	0.1742	0.7798	0.002*
Diet	0.00001*	0.911	0.958	0.970	0.855	0.830	0.0098*	0.5648	0.007*
Surgery×treatment	0.054	0.012*	0.006*	0.134	0.888	0.431	0.702
Surgery×diet	-	0.337	0.976	0.252	0.792	0.498	0.090
Treatment×diet	-	0.280	0.835	0.075	0.906	0.054	0.8049	0.2976	0.024*
Surgery×treatment×diet	-	0.919	0.899	0.948	0.332	0.516	0.176

Table summarizes the different *P* values obtained by 2-way ANOVA in the 25(OH)D, creatinine and urea-dependent variables and 3-way ANOVA for the other dependent variables. *Differences were considered statistically significant for *P*<0.05.

Results

Characterization of Uremia and Vitamin D Deficiency on Blood Chemistry

Figure 1A shows the experimental design of a combined model of 3/4 nephrectomy (CKD) with vitamin D deficiency²⁵ and the corresponding controls (non-CKD). Serum concentrations of urea and creatinine increased 2- (5.5±0.8–11.9±2.4 mmol/L) to 3-fold (15.4±1.7–44.3±8.9 μmol/L), respectively, 3 weeks following surgery, and this was stable for the remainder of the experiment (Figure 1B and 1C). No significant differences on the degree of renal failure were observed among the 4 CKD groups at the end point (Figure S1A and S1B). Three weeks after the induction of vitamin D deficiency, the average of 25(OH)D and 1,25(OH)₂D concentrations were below the detection levels (8 nmol/L and 20 pmol/L, respectively) in most of the animals exposed to the vitamin D-deficient diet (Figure 1D and 1E; *P*<0.0001 for diet by 2-way ANOVA). Moreover, the influence of 3/4 nephrectomy was confirmed by 2-way ANOVA (*P*<0.01 for surgery) where CKD animals with standard diet showed a higher concentration of 25(OH)D (92.93±24.8 nmol/L) and a lower 1,25(OH)₂D (187.8±33.1 pmol/L) when compared with non-CKD animals with standard diet (25(OH)D, 70.92±18.97 nmol/L; 1,25(OH)₂D, 244.9±46.78 pmol/L). Thus, serum measurements confirmed the induction of uremia and vitamin D deficiency.

In addition, we investigated whether paricalcitol treatment affected serum PTH levels. When analyzing the overall effect of 3/4 nephrectomy on PTH levels, a significant increase in uremic animals was found, when compared with non-CKD (Figure S1C). When comparing individual groups, the significant influence of surgery was confirmed by 3-way ANOVA (*P*<0.01; Figure S1D). Furthermore, PTH concentrations were

significantly affected by treatment and diet (*P*<0.01 in both cases), with effects differing between groups. Specifically, paricalcitol treatment reduced PTH concentrations in vitamin D-deficient CKD animals (261.5±80.1 untreated and 98±69.2 pg/mL treated), with no significant effect in other groups (*P*=0.024 for treatment×diet).

Paricalcitol Treatment Attenuates Uremia-Induced Endothelial Damage in Thoracic Aorta

To explore the effects of uremia and vitamin D deficiency on aortic endothelial permeability, animals were injected intravenously with Evans Blue dye 30 minutes before being euthanized. CKD was confirmed to have a significant effect on vascular permeability by a 3-way ANOVA (*P*<0.01 for surgery). The permeability of the aortic endothelium was increased (53%) in untreated CKD animals on standard diet when compared with non-CKD controls (Figure 2A). A similar trend (43% increase in Evans Blue penetrance) was observed for nontreated uremic vitamin D-deficient animals compared with non-CKD animals. Endothelial permeability was normalized in CKD animals treated with paricalcitol, irrespective of the diet (Figure 2A; *P*=0.021 for treatment; *P*=0.012 for surgery×treatment). No changes were observed in non-CKD animals irrespective of both diet and treatment. To further support the findings on Evans Blue extravasation, the surface perimeter of the aorta was examined for endothelial gaps, which are an anatomic correlate of the permeability of the aortic endothelium (Figure 2B; enlargements). CKD animals without paricalcitol treatment showed an increment (13.6%–13.8%) of the endothelial gaps (Negative CD31 surface (μm) × 100/μm total CD31) in good agreement with the data of the Evans Blue penetration (Figure 2C; *P*<2⁻¹⁶ for surgery).

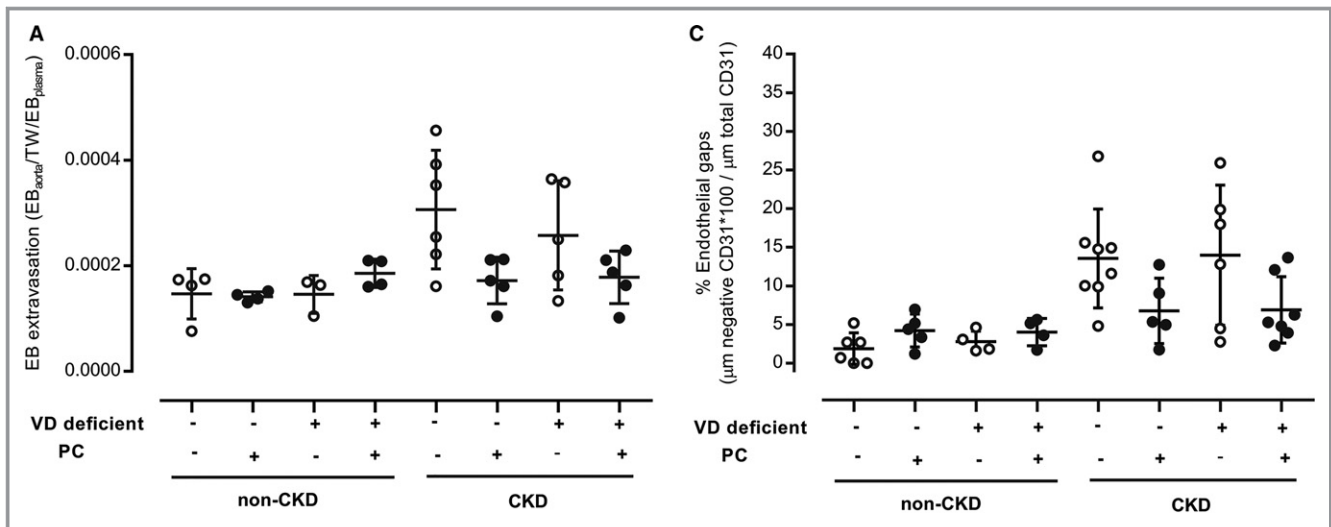


Figure 2. Paricalcitol ameliorates uremic-induced endothelial dysfunction. A, Quantification of formamide-extracted Evans Blue (EB; EB tissue ($\mu\text{g}/\text{mL}$)/tissue weight (TW; mg)/EB plasma $\mu\text{g}/\text{mL}$) in thoracic aorta corrected for tissue weight and the Evans Blue plasma concentration (CKD indicates uremic animals; non-CKD, nonuremic animals; PC, paricalcitol; and VD, vitamin D). $P=0.003$ for surgery, $P=0.021$ for treatment, $P=0.911$ for diet, $P=0.012$ for surgery \times treatment. B, Representative images of immunohistochemistry of thoracic aorta sections stained with CD31 antibody. Images represent 1 rat per group. Scale bars are 100 μm , magnification: 20 \times . Enlargements of the white boxes are included on the bottom of every figure. $P=2 \times 10^{-16}$ for surgery, $P=0.041$ for treatment, $P=0.958$ for diet, $P=0.006$ for surgery \times treatment. C, Graph shows percentage of endothelial gaps measured on 3 sections of the aortic tissue (μm of CD31 negative surface $\times 100 / \mu\text{m}$ total surface measured CD31). Data are represented as means \pm SD ($n=4-7$). Differences were considered statistically significant for $P<0.05$ using 3-way ANOVA. D, Correlation between EB extravasation and % of endothelial gaps (Pearson regression; $P<0.05$; $n=33$).

Paricalcitol treatment rescued these differences and protected against endothelial damage in CKD animals with both standard and vitamin D–deficient diet ($P=0.041$ for treatment). Subsequently, 3-way ANOVA analysis confirmed that the effect of surgery on endothelial damage is dependent on the type of treatment provided to the animals ($P=0.006$ for surgery \times treatment) while no significant 2 and 3 interactions were detected with the diet. In addition, a positive Pearson correlation ($r=0.475$, $P=0.0051$) was found between the amount of Evans Blue extravasation and the percentage of endothelial gaps, suggesting a direct relationship between these 2 parameters (Figure 2D). Thus, we demonstrate that CKD drives aortic endothelial leakage and dysfunction independently from endogenous 25(OH)D status, whereas paricalcitol improves the integrity of the endothelium from uremia-induced barrier loss.

Endothelial Changes Are Partially Associated With Serum α -Klotho Levels

To determine if alterations in endothelial integrity are possibly mediated by α -Klotho, gene expression and protein abundance of α -Klotho were first examined in kidney tissue (Figure S2). When testing the overall effect of uremia on α -Klotho, we observed that CKD leads to a significant downregulation (by 40%) of both α -Klotho protein and mRNA

levels when compared with non-CKD animals (Figure 3A and 3C). After comparing individual groups, 3-way ANOVA analysis confirmed that surgery had a significant influence in α -Klotho protein ($P<2^{-16}$) and mRNA levels ($P=0.001$), while no differences were found when animals were challenged with a standard or vitamin D–deficient diet. Furthermore, no effect was detected after paricalcitol supplementation (Figure 3B and 3D). In accordance with the results in the kidney, we found a statistically significant effect of CKD on α -Klotho serum concentrations (50% decrease) when comparing all CKD with non-CKD animals (Figure 3E). When evaluating the effect of paricalcitol on serum α -Klotho, there was a trend in both non-CKD (10.7 ± 3.1 versus 23.8 ± 7.1 pg) and CKD groups (4.8 ± 2.0 versus 10.2 ± 8.6 pg) with standard diet, whereas no influence was detected in the vitamin D–deficient groups. Three-way ANOVA analysis showed a significant independent effect from surgery on soluble α -Klotho ($P=0.001$), while treatment displayed a borderline effect, both independently ($P=0.051$) and together with diet ($P=0.054$ for treatment \times diet). Together, these findings indicate that CKD leads to α -Klotho deficiency in kidney tissue, whereas no effect was observed for vitamin D status. Although α -Klotho levels were not restored by paricalcitol treatment, we cannot exclude the possibility that α -Klotho contributed to the vasoprotective effect observed in uremic animals.

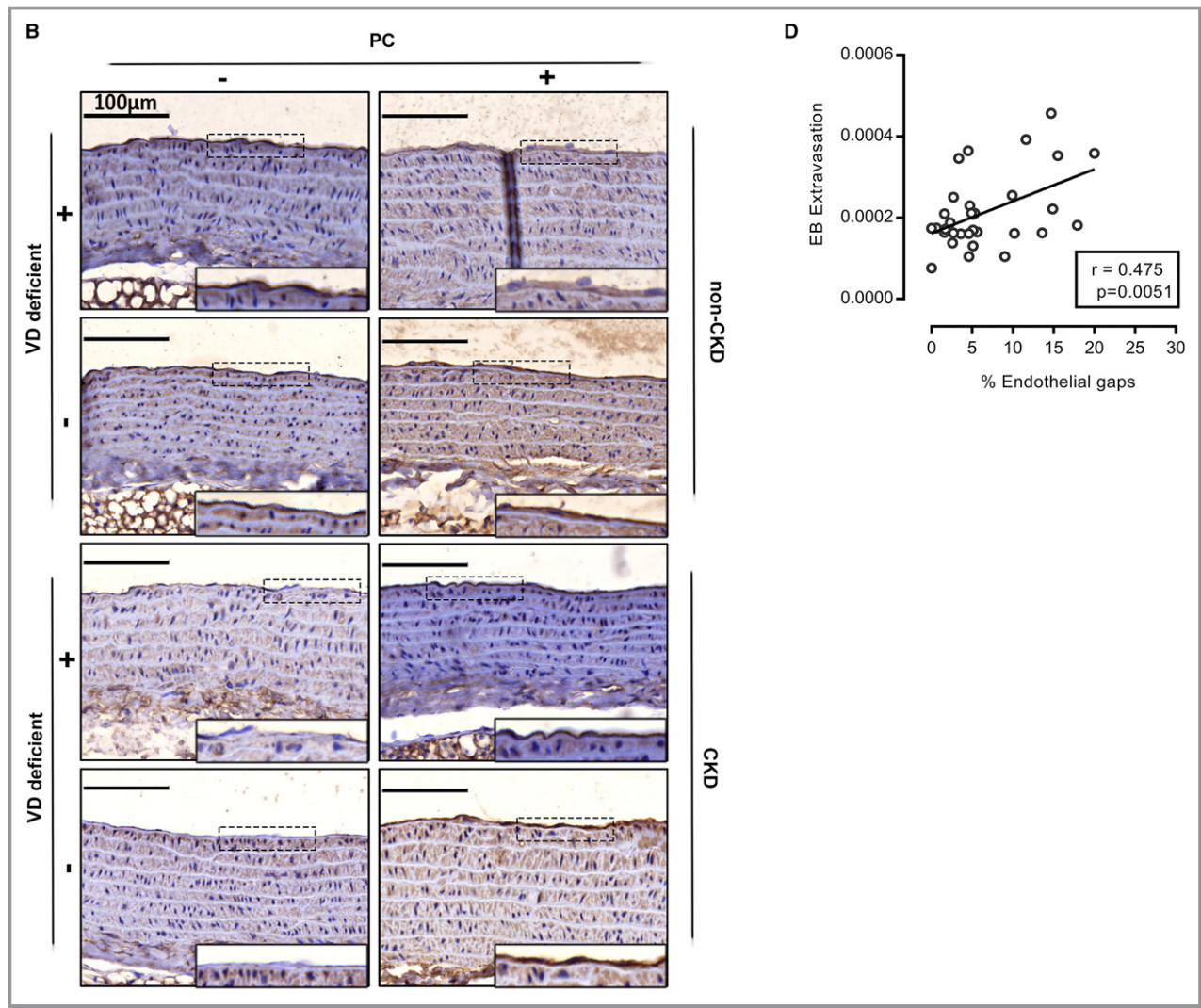


Figure 2. Continued.

Paricalcitol Stabilizes Basal Human Endothelial Barrier Function

To investigate the direct effects of paricalcitol and α -Klotho on endothelial integrity, in vitro studies focused on the real-time changes in barrier function measured by electric cell-substrate impedance sensing.²⁷ Paricalcitol (100 nmol/L) effectively increased (8.4%) the absolute basal endothelial resistance after 24-hour exposure. No significant impact on the basal endothelial barrier function was detected 24 hours after the addition of α -Klotho (400 pM; 4.3%), nor for the lower dose of paricalcitol (10 nmol/L; 5.3%) when compared with control (Figure 4A). Based on our current findings, we proceeded by evaluating whether the distribution of the main adherens junction protein VE-cadherin, a determinant of endothelial junctional stability,²⁹ and F-actin rearrangement could explain the changes of endothelial barrier enhancements. Immunostaining for VE-cadherin revealed that

paricalcitol significantly enhanced its peripheral localization in a dose-dependent manner (39% for 10 nmol/L and 48% for 100 nmol/L) compared with control conditions (Figure 4B and 4C). In addition, the F-actin content was found to be significantly strengthened and more densely arranged in the cortical area of paricalcitol-stimulated (100 and 10 nmol/L) HUVECs, while controls showed a normal F-actin distribution (Figure 4D). α -Klotho-treated HUVECs showed no changes for VE-cadherin and F-actin intensity. Thus, these findings suggest that paricalcitol modulates endothelial barrier enhancement by enforcement of junctional VE-cadherin and the cortical F-actin cytoskeleton.

Paricalcitol Attenuates Endothelial Dysfunction Following Barrier-Disruptive Agents

To further test whether paricalcitol and α -Klotho contribute to the stabilization and restoration of reduced endothelial

integrity induced by a challenge, we analyzed HUVECs in an electric wounding assay.²⁷ The restoration of endothelial resistance for paricalcitol 100 nmol/L in this wound-healing assay was significantly higher compared with control, as reflected by the slope of the recovery after wounding (140.7 ± 7.5 versus 116.3 ± 11.5 a.u.) and the area under the curve starting from 1 hour (5651 ± 88.33 versus 5158 ± 154.4 a.u.) (Figure 5A and 5C). Next, using thrombin

as a pro-permeability factor,³⁰ we evaluated the capacity of paricalcitol and α -Klotho in preventing the endothelial permeability and gap formation. In accordance with the wound assay, paricalcitol attenuated thrombin-induced endothelial dysfunction as shown by a 35% (100 nmol/L) and 38% (10 nmol/L) reduction of the resistance after 1 hour of thrombin as compared with the control, which showed a 45% reduction induced by thrombin (Figure 5D and 5E). The

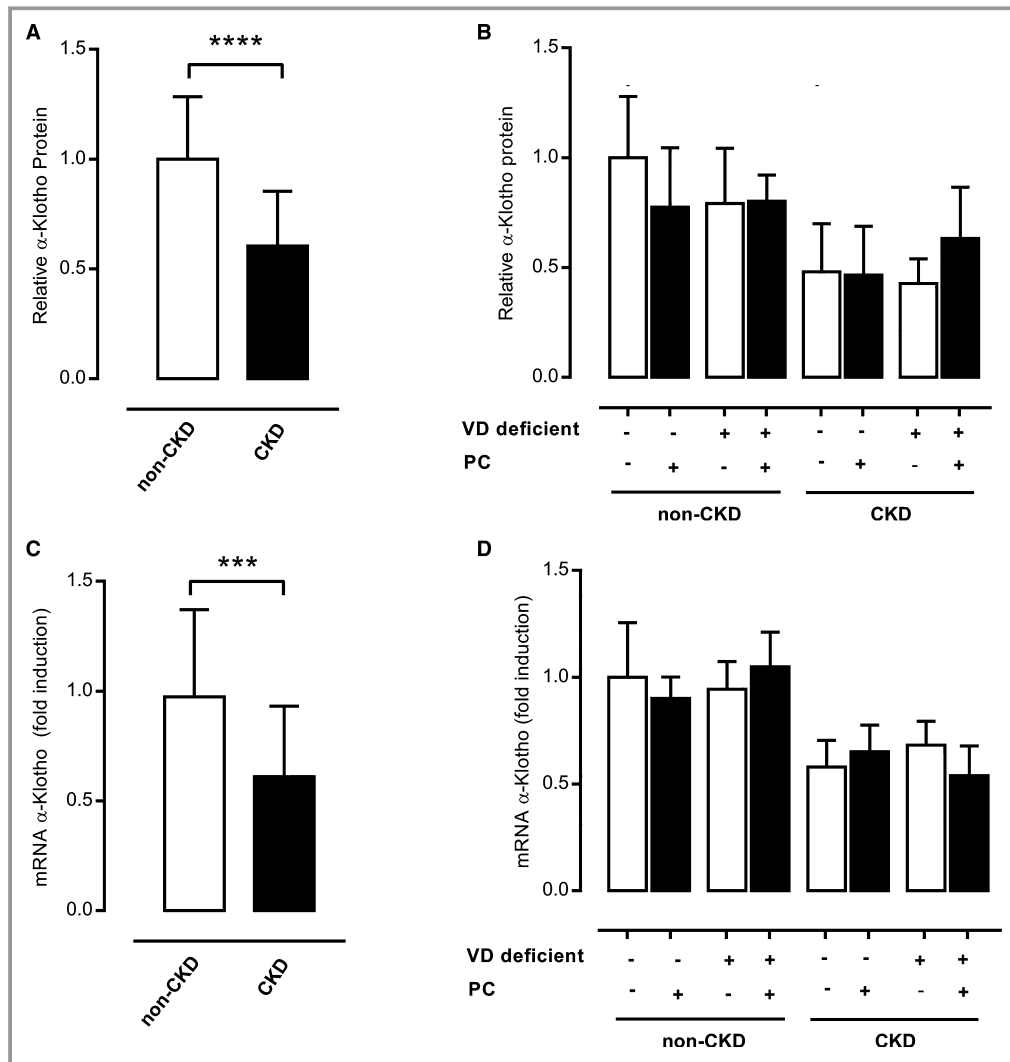


Figure 3. Effect of paricalcitol on α -Klotho levels in kidney tissue and in the circulation. Quantification of α -Klotho protein (α -Klotho/glyceraldehyde 3-phosphate dehydrogenase) normalized to control group in kidney tissue (respective immunoblot is shown in Figure S2) of non-CKD and CKD animals pooled (A, $n=23-27$) and not pooled groups (B, $n=6-8$). $P=2\times 10^{-16}$ for surgery, $P=0.935$ for treatment, $P=0.970$ for diet. Relative mRNA expression of α -Klotho was assessed by quantitative polymerase chain reaction in kidney tissue of pooled (C, $n=23-28$) and nonpooled (D, $n=6-8$) groups. B-Actin was used as housekeeping gene. $P=0.001$ for surgery, $P=0.881$ for treatment, $P=0.855$ for diet serum α -Klotho (week 11) was measured by the immunoprecipitation-immunoblotting assay (E, pooled samples $n=22-24$) and (F, separate groups $n=5-7$). $P=0.001$ for surgery, $P=0.051$ for treatment, $P=0.830$ for diet (CKD indicates uremic animals; VD, vitamin D; non-CKD, nonuremic animals; and PC, paricalcitol). Data are represented as means \pm SD. Differences were considered statistically significant for $P<0.05$ using unpaired t test for A, C, E and 3-way ANOVA for B, D, F. ** $P<0.01$, *** $P<0.001$, **** $P<0.0001$.

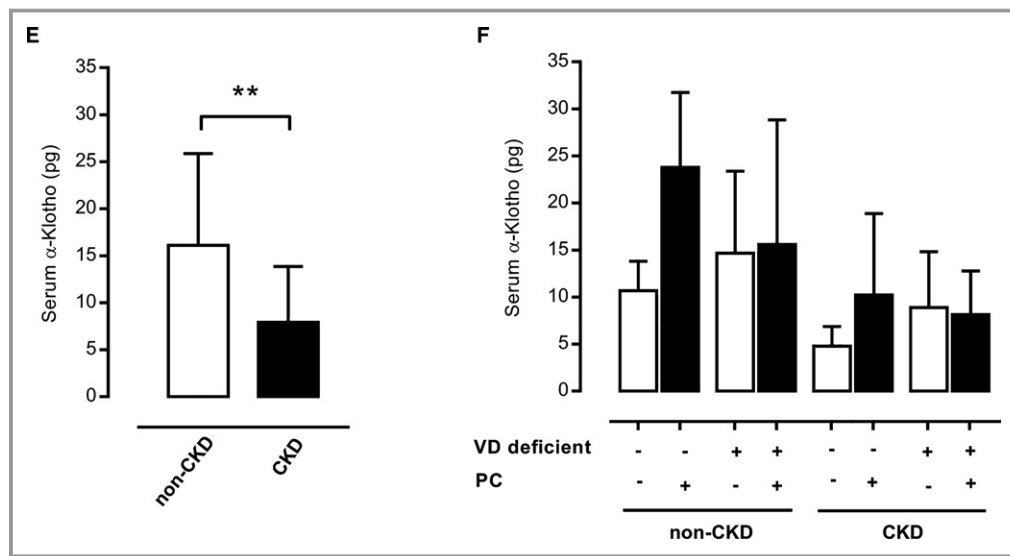


Figure 3. (Continued)

area under the curve of normalized data from baseline after the addition of thrombin was significantly higher for HUVECs prestimulated with paricalcitol 100 nmol/L as compared with the control (3.35 ± 0.14 versus 2.96 ± 0.07 a.u.) (Figure 5F). There was a small, statistically nonsignificant effect during the recovery phase for α -Klotho prestimulated HUVECs (43% drop; 3.20 ± 0.18 a.u.). Finally, using immunofluorescent detection of VE-cadherin and F-actin fibers, we could confirm that paricalcitol attenuated the thrombin-induced intercellular gap formation after 60 minutes and 120 minutes, which is in line with the real-time measurements of the barrier function (Figure 5G).

The induction of F-actin stress fibers upon 60 minutes of thrombin stimulation was not prevented by paricalcitol although, after 120 minutes, cells showed a more densely packed cortical F-actin ring (Figure 5G). Taken together, these findings indicate that paricalcitol strengthened the endothelial barrier during disruptive conditions accompanied by enhanced endothelial migration and limited the interendothelial cell gap formation. We observed no statistically significant effect of α -Klotho-treated cells, whereas paricalcitol confirmed distinct beneficial contributions to the maintenance of the endothelial barrier integrity.

Discussion

Our study demonstrates that CKD induces endothelial cell disruption in the thoracic aorta *in vivo* and that this can be attenuated by paricalcitol, an active vitamin D analogue. This conclusion is based on a striking parallel between Evans Blue penetration into the aortic wall and the detachment of endothelial cells from the aorta, both pathological features that normalized after administration of paricalcitol.

Importantly, baseline vitamin D status, both active and nutritional, did not play a role in these effects. Originally, we hypothesized that presumed protection of paricalcitol was mediated by an increment of circulating α -Klotho.³¹ Although our data do suggest some increase in circulating α -Klotho following paricalcitol administration in vitamin D-sufficient animals, this increase was not statistically significant. However, this does not exclude that α -Klotho did contribute to vasoprotection in our uremic model. Finally, we confirmed *in vitro* that paricalcitol enforces endothelial cell-cell adhesions and thereby the endothelial monolayer integrity. This feature most likely prevents the interendothelial gap formation seen *in vivo* by enhancing the restoration of the endothelial barrier following disruptive hits, suggesting that paricalcitol was the principal mediator of the endothelial stability following uremia.

Limited previous findings pointed to abnormal endothelial cell properties in CKD, contributing to cardiovascular complications in patients.³ Although the underlying mechanistic pathway that might explain the loss of endothelial barrier function in CKD has been unclear so far, it was suggested that vitamin D deficiency might participate in this uremia-induced phenomenon.^{6,32} Here, we found that vitamin D deficiency induced in our recently developed rat model²⁵ did not aggravate the injury on the aortic endothelial layer caused by CKD. Despite these findings, supplementation with the active vitamin D analogue paricalcitol did result in amelioration of the aortic endothelial permeability and limited the gap formation observed in CKD rats. In line with our results, Wu-Wong et al have reported that paricalcitol can improve endothelial-dependent relaxation in uremic rats independent from effects on PTH serum concentration.^{16,17} Recently, randomized clinical trials conducted in patients with CKD also demonstrated that

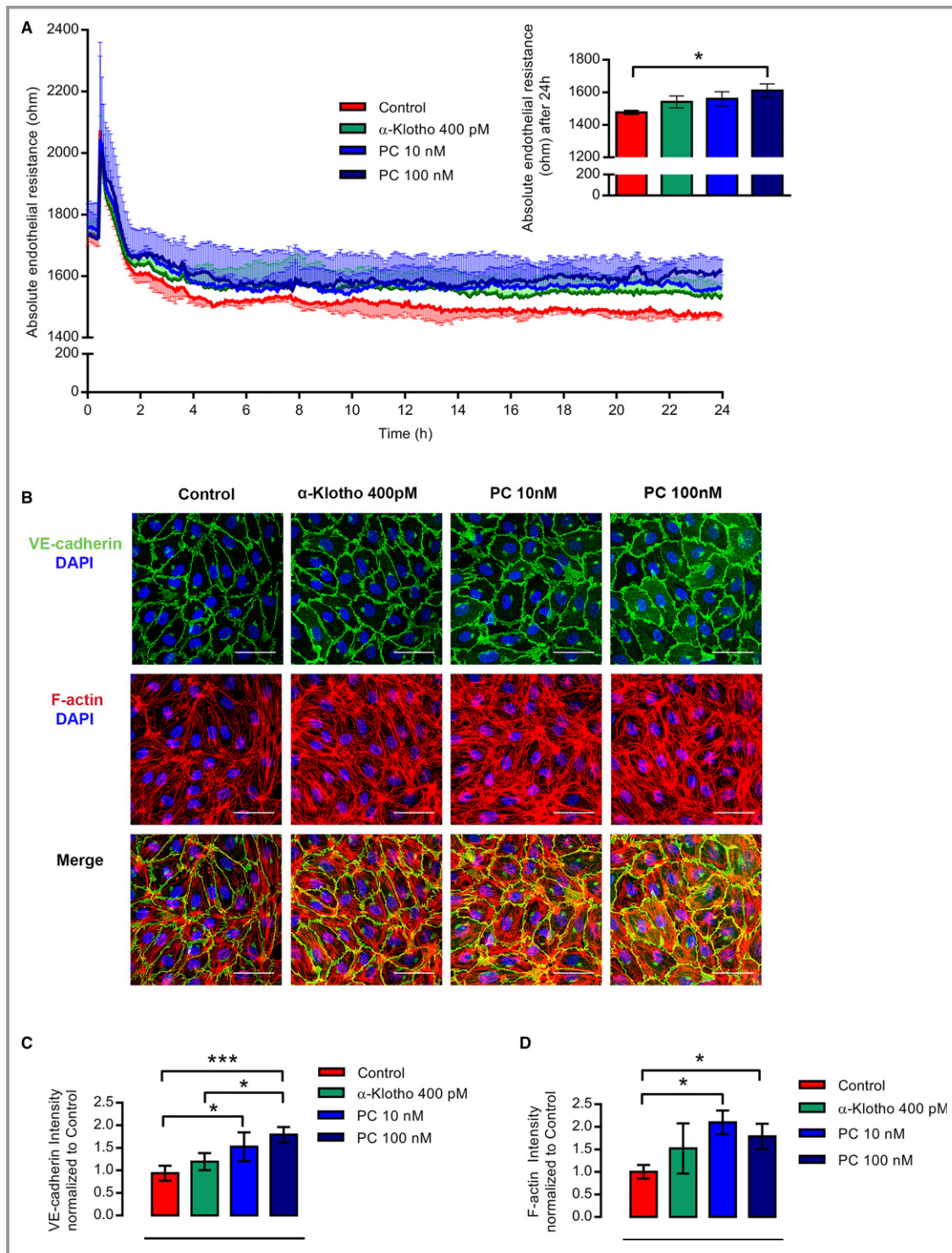


Figure 4. The role of paricalcitol and α -Klotho on basal endothelial barrier function. A, Representative time-course of the absolute endothelial electrical resistance of a HUVEC monolayer during 24 hours of stimulation. Upon confluence, the cells have been stimulated with different conditions in basal medium plus 1% human serum albumin. Insert: Quantification of the absolute endothelial resistance (ohm) after 24 hours of stimulation (PC indicates paricalcitol). Results represent the mean \pm SD of n=3 (from cells of 3 donors) from 1 of 3 representative experiments. B, Representative VE-cadherin (green) and F-actin (red) and nuclei (blue) immunostaining of HUVECs after 24 hours of stimulation in basal medium plus 1% human serum albumin. Scale bar represents 50 μ m. Magnification, 63 \times . The corresponding intensity (mean) quantification of 3 independent experiments normalized to control is represented in the graphs for of VE-cadherin (C) and F-actin (D), respectively. Data show means \pm SD. Differences were considered statistically significant for $P < 0.05$ using 1-way ANOVA. * $P < 0.05$, *** $P < 0.001$.

treatment with active vitamin D leads to significantly favorable changes in endothelial function.^{18,19,33–35}

In accordance with our *in vivo* findings, we confirmed the potency of paricalcitol as an endothelial barrier function stabilizer in HUVECs by electric cell-substrate impedance sensing.²⁷ Further, paricalcitol was found to enhance recovery from endothelial disruptive hits such as an electric wound (simulating an injury in the endothelium) or thrombin (to induce permeability and gap formation).^{27,30} Interestingly, this effect was mediated by enhanced intercellular junctions resembling a protective mechanism previously reported in brain endothelial cells where active vitamin D preserved the barrier integrity following hypoxia.³⁶ Here, we found that paricalcitol strengthened the adherens junction protein VE-cadherin in HUVECs, an endothelium-specific homotypic adhesion protein essential to control the integrity of the endothelial monolayer.²⁹ In addition, VE-cadherin interacts, via other proteins, with the F-actin cytoskeleton to orchestrate the cell-cell contact and thus maintaining barrier function.³⁷ Our data show that paricalcitol stabilizes the cortical F-actin ring formation, which is necessary for the maintenance of a quiescent endothelium.³⁷ After thrombin addition, there is a reorganization of the cortical actin ring as a requirement for interendothelial gap formation.³⁰ Interestingly, immunofluorescent imaging revealed that HUVECs, prestimulated with paricalcitol, displayed less gap formation upon thrombin, which is in line with the barrier function studies. These endothelial protective effects could be mediated by changes in matrix metalloproteinase 9 concentrations. As recently demonstrated, active vitamin D can reduce matrix metalloproteinase 9 expression in brain endothelial cells and prevent the hypoxia-mediated loss of cell-cell contact.³⁶ Our observations are in line with previous studies where active vitamin D preserved the integrity of intestinal mucosal barrier and stimulated epithelial cell migration.³⁸ Together, our findings suggest that paricalcitol limits uremia-induced endothelial damage by enhancing endothelial barrier integrity and recovery capacity following a disruptive hit. Furthermore, although adherens junctions were not examined in the *in vivo* study, we suggest that endothelial cell detachment and permeability observed in aortic tissue was attenuated by enforced VE-cadherin in paricalcitol treated rats.

Instead of a direct effect on target tissue, as an alternative explanation for beneficial effects of active vitamin D, it has been postulated that it can upregulate renal α -Klotho as the actual effector of remote beneficial effects, after shedding its ectodomain.^{20,21,39,40} Indeed, α -Klotho deficiency in mice leads to a limited vasodilatory response and increased permeability in the endothelial cells among other vascular complications also observed in CKD patients.^{22–24,41} As reported previously in other uremic *in vivo* models^{20,21} and CKD patients,^{42,43} we confirmed that impaired kidney function induced downregulation of mRNA and α -Klotho protein levels

in kidney tissue accompanied by lower serum concentrations. However, it was unexpected that neither vitamin D deficiency nor paricalcitol supplementation affected α -Klotho in the kidney tissue or its concentration in serum. Only in paricalcitol-treated, vitamin D-sufficient animals, a nonsignificant trend was noted. Consistent with this suggestion of increase, Lau et al found, in intraperitoneally paricalcitol (100 and 300 ng/kg) treated uremic mice on a high-phosphate diet, increased serum α -Klotho concentrations despite unchanged kidney tissue expression, leaving the origin of the increment elusive.²⁰ In this experiment, we applied similar paricalcitol concentrations (100 ng/kg) as in that study and mimicked the clinical setting by applying an oral, instead of intraperitoneal, route of administration, which might have limited the efficacy on serum α -Klotho concentrations in our animal model.

Although our experiments do not support a protective effect of α -Klotho on the aortic endothelium, this cannot be completely ruled out either. In previous experimental *in vitro* studies, the α -Klotho protein was found to suppress oxidative stress in the endothelium, to increase nitric oxide production and to limit endothelial permeability by the internalization of both vascular endothelial growth factor receptor-2 and transient receptor potential 1.^{31,44} Moreover, other experimental studies found an endothelium-protective effect by overexpression of α -Klotho in endothelial cells⁴⁵ or application of culture media from α -Klotho-expressing cells.⁴⁴ Here, when we applied an effective exogenous α -Klotho concentration (400 pM) in the *in vitro* parts of our study as previously reported,^{46,47} we observed a statistically nonsignificant trend of the basal endothelial barrier function. However, this effect was limited when compared with paricalcitol effects, suggesting that the active vitamin D analog was the more important mediator.

Our study has some limitations. While we applied established experimental models of uremia and vitamin D deficiency, the experimental design did not include sham surgery for non-CKD animals, so we cannot exclude that some differences are the consequences of the surgery itself and not of kidney failure. Based on the study duration, however, and our experience when developing the model, we consider it highly unlikely that differences between the groups are based on anything else than differences in kidney function, and decided to limit animal discomfort for the control group. Another possible limitation is that we administered paricalcitol orally, making bioavailability less predictable. However, on the basis of the PTH-suppressive effect and the effect on our primary read-outs, we think this was of limited relevance and may only lead to underestimation of the true effect. Similarly, it might have been of interest to determine whether changes

in the renin-angiotensin system and blood pressure could partially explain the results observed in the uremic model, as active vitamin D suppresses renin, which in turn may have an effect on the endothelium. Despite these limitations, the beneficial effects of paricalcitol in the in vitro setup are unlikely to be explained by effect-mediation of renin suppression by paricalcitol. In addition, we cannot exclude the possibility that the beneficial effects of paricalcitol on the endothelium are related to a local increment of α -Klotho. More research is required to determine the influence of α -Klotho during active vitamin D-mediated endothelial protection. Finally, electric wound and thrombin were used to simulate endothelial injury and

permeability detected in rat aortic endothelium and evaluate paricalcitol's and α -Klotho's protective capacities. However, these 2 approaches provide a close, but incomplete, estimation of the damage exerted by uremia in the endothelium. Moreover, the results were similar for these 2 different forms of endothelial injury.

Because of recent negative results from clinical trials in patients with CKD that aimed to improve cardiac function (PRIMO [Paricalcitol Capsule Benefits in Renal Failure-Induced Cardiac Morbidity] and OPERA), enthusiasm to use active vitamin D was dampened because of the obviously slightly higher risk for hypercalcemia. However, nihilism about potential benefits of the clinical use of active vitamin D seems

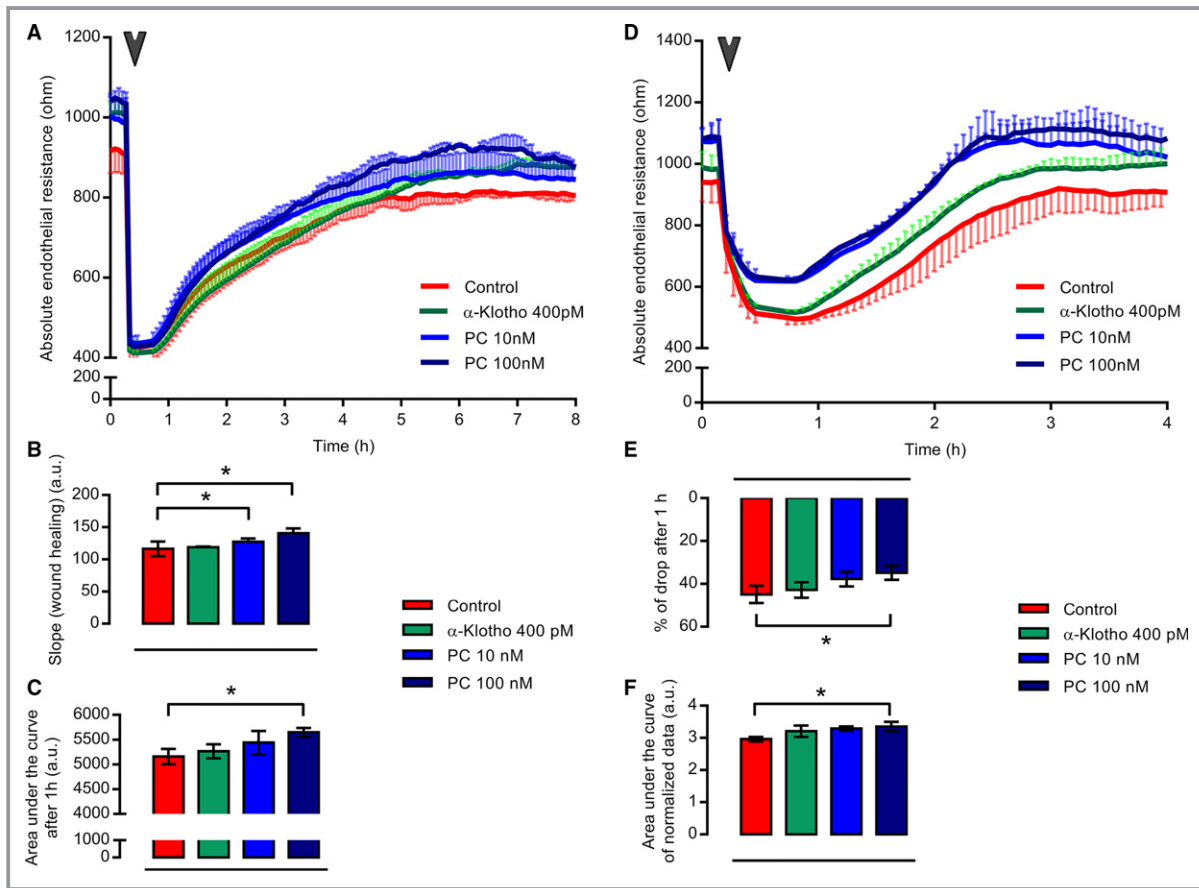


Figure 5. Paricalcitol protects against endothelial barrier dysfunction. A, Representative time course absolute endothelial electrical resistance measurements of HUVEC monolayers during migration after 24 hours of stimulation in basal medium plus 1% human serum albumin. Arrow indicates the induction of an electrical wound. B and C, Quantification of the wound healing capacities are represented as the slope of the curves (1–3 hours; a.u.) and the area under the curve (a.u.) measured from 1 hour onwards. D, Representative absolute endothelial electrical resistance of HUVEC monolayers upon thrombin stimulation in basal medium plus 1% HSA. Arrow indicates the addition of thrombin (1 U/mL). E through G, Quantification of the response of thrombin by calculating the drop in resistance (%) after 1 hour of stimulation and the area under the curve (a.u.) after normalizing the data at 0 hour. Data represent the mean±SD of n=3 (from cells of 3 donors) from 1 of 3 representative experiments. Differences were considered statistically significant for $P<0.05$ using 1-way ANOVA. * $P<0.05$. F, Effects of paricalcitol (PC) 100 nmol/L on endothelial barrier function under basal (0 minutes) and thrombin response (60 minutes and 120 minutes) are shown on the immunofluorescence images of the VE-cadherin (green), F-actin (red) and the nuclei (blue). Scale bars are 50 μ m. Magnification, 63 \times . Enlargements of the white boxes are showed on the bottom. Images are representative for 1 of 3 experiments performed independently.

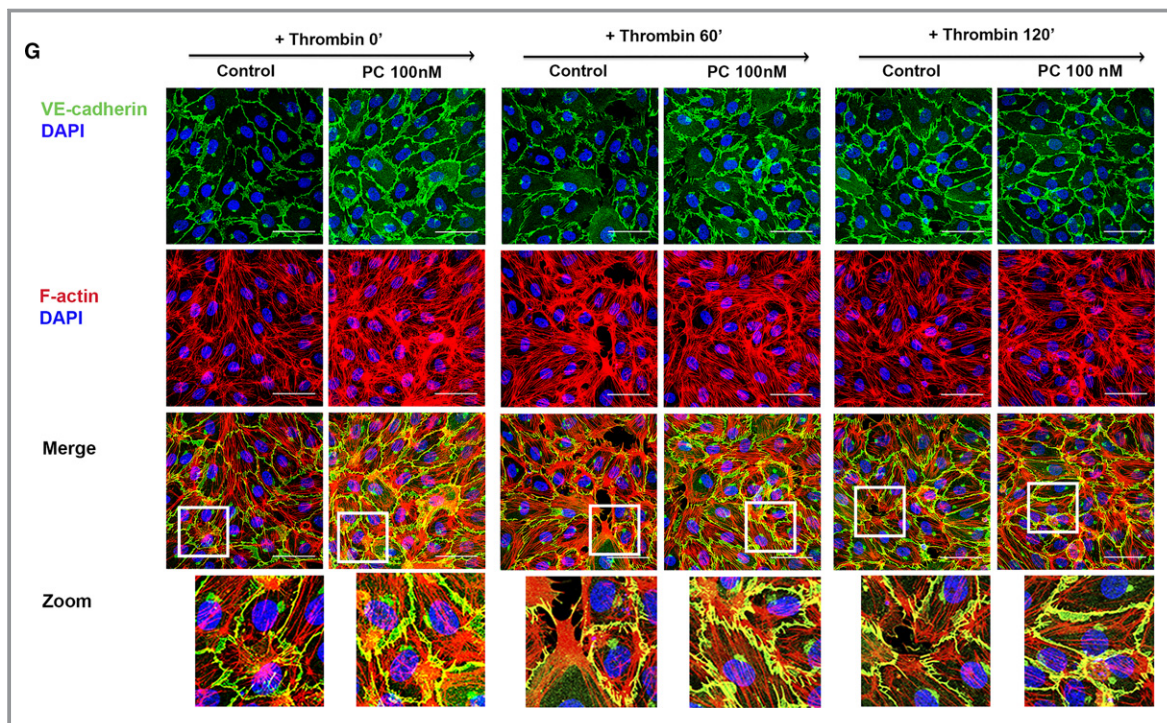


Figure 5. (Continued)

inappropriate. Collectively, we demonstrated a consistent, protective effect of the oral use of paricalcitol on uremia-induced endothelial disruption. Although α -Klotho has been suggested to be an important mediator of endothelial cell stability, we could not demonstrate its role in the paricalcitol-mediated vasoprotective effects. Alternatively, we provide evidence that paricalcitol directly maintains endothelial barrier integrity by enhancing the cell-to-cell contacts. Clinically, this benefit may translate into improved vascular health in patients with CKD.

Acknowledgments

We thank UT Southwestern George M. O'Brien Kidney Research Core Center (P30DK079328), Texas, services for soluble α -Klotho measurements. We thank Jeroen Kole and Dr Renee Musters (VU University Medical Center Amsterdam, Advanced Optical Microscopy Core facility, The Netherlands) for their help with the microscope equipment.

Sources of Funding

This work was supported by a grant from Abbvie Laboratories (REN-12-0011).

Disclosures

Vervloet reports grants from AbbVie, during the conduct of the study, and grants from Amgen, personal fees from

Amgen, personal fees from VFMCRC, grants from FMC, personal fees from Otsuka, personal fees from Medice, personal fees from BBraun, and personal fees from Baxter, outside the submitted work. The remaining authors have no disclosures to report.

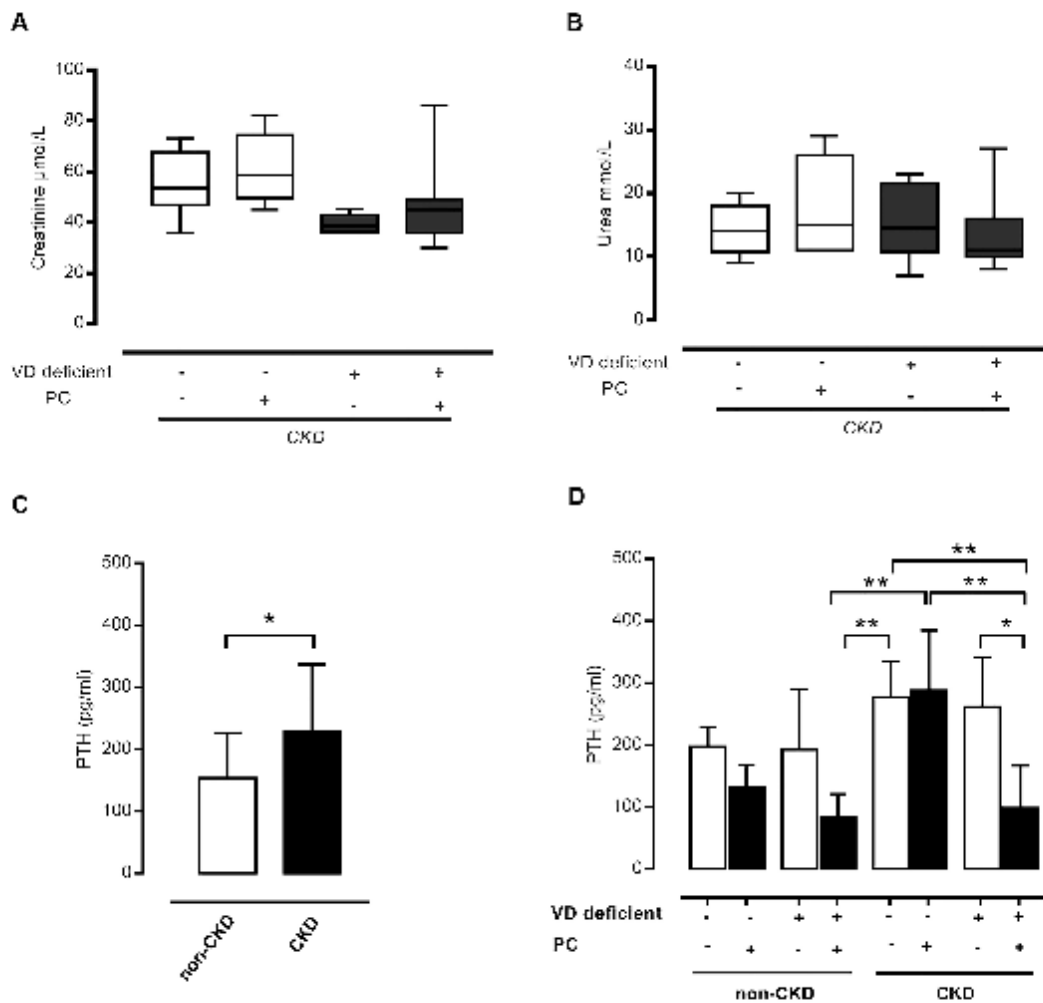
References

- Schiffrin EL, Lipman ML, Mann JF. Chronic kidney disease: effects on the cardiovascular system. *Circulation*. 2007;116:85–97.
- Malyszko J. Mechanism of endothelial dysfunction in chronic kidney disease. *Clin Chim Acta*. 2010;411:1412–1420.
- Moody WE, Edwards NC, Madhani M, Chue CD, Steeds RP, Ferro CJ, Townend JN. Endothelial dysfunction and cardiovascular disease in early-stage chronic kidney disease: cause or association? *Atherosclerosis*. 2012;223:86–94.
- de Borst MH, Vervloet MG, ter Wee PM, Navis G. Cross talk between the renin-angiotensin-aldosterone system and vitamin D-FGF-23-klotho in chronic kidney disease. *J Am Soc Nephrol*. 2011;22:1603–1609.
- Hu MC, Shiizaki K, Kuro-o M, Moe OW. Fibroblast growth factor 23 and Klotho: physiology and pathophysiology of an endocrine network of mineral metabolism. *Annu Rev Physiol*. 2013;75:503–533.
- Santoro D, Pellicanò V, Cernaro V, Lacava V, Lacquaniti A, Atteritano M, Buemi M. Role of vitamin D in vascular complications and vascular access outcome in patients with chronic kidney disease. *Curr Med Chem*. 2016;23:1698–1707.
- Seiler S, Rogacev KS, Roth HJ, Shafein P, Emrich I, Neuhaus S, Floege J, Fliser D, Heine GH. Associations of FGF-23 and sKlotho with cardiovascular outcomes among patients with CKD stages 2–4. *Clin J Am Soc Nephrol*. 2014;9:1049–1058.
- Gonzalez-Parra E, Rojas-Rivera J, Tuñón J, Praga M, Ortiz A, Egido J. Vitamin D receptor activation and cardiovascular disease. *Nephrol Dial Transplant*. 2012;27(suppl 4):iv17–iv21.
- Bodyak N, Ayus JC, Achinger S, Shivalingappa V, Ke Q, Chen YS, Rigor DL, Stillman I, Tamez H, Kroeger PE, Wu-Wong RR, Karumanchi SA, Thadhani R, Kang PM. Activated vitamin D attenuates left ventricular abnormalities induced by dietary sodium in Dahl salt-sensitive animals. *Proc Natl Acad Sci U S A*. 2007;104:16810–16815.

10. Wang AY, Fang F, Chan J, Wen YY, Qing S, Chan IH, Lo G, Lai KN, Lo WK, Lam CW, Yu CM. Effect of paricalcitol on left ventricular mass and function in CKD—the OPERA trial. *J Am Soc Nephrol*. 2014;25:175–186.
11. Thadhani R, Appelbaum E, Pritchett Y, Chang Y, Wenger J, Tamez H, Bhan I, Agarwal R, Zoccali C, Wanner C, Lloyd-Jones D, Cannata J, Thompson BT, Andress D, Zhang W, Packham D, Singh B, Zehnder D, Shah A, Pachika A, Manning WJ, Solomon SD. Vitamin D therapy and cardiac structure and function in patients with chronic kidney disease: the PRIMO randomized controlled trial. *JAMA*. 2012;307:674–684.
12. Molinari C, Uberti F, Grossini E, Vacca G, Carda S, Invernizzi M, Cisarì C. 1 α ,25-Dihydroxycholecalciferol induces nitric oxide production in cultured endothelial cells. *Cell Physiol Biochem*. 2011;27:661–668.
13. Stach K, Kälsch AI, Nguyen XD, Elmas E, Králev S, Lang S, Weiss C, Borggreve M, Kälsch T. 1 α ,25-dihydroxyvitamin D3 attenuates platelet activation and the expression of VCAM-1 and MT1-MMP in human endothelial cells. *Cardiology*. 2011;118:107–115.
14. Mizobuchi M, Finch JL, Martin DR, Slatopolsky E. Differential effects of vitamin D receptor activators on vascular calcification in uremic rats. *Kidney Int*. 2007;72:709–715.
15. Panizo S, Barrio-Vázquez S, Naves-Díaz M, Carrillo-López N, Rodríguez I, Fernández-Vázquez A, Valdivielso JM, Thadhani R, Cannata-Andía JB. Vitamin D receptor activation, left ventricular hypertrophy and myocardial fibrosis. *Nephrol Dial Transplant*. 2013;28:2735–2744.
16. Wu-Wong JR, Li X, Chen YW. Different vitamin D receptor agonists exhibit differential effects on endothelial function and aortic gene expression in 5/6 nephrectomized rats. *J Steroid Biochem Mol Biol*. 2015;148:202–209.
17. Wu-Wong JR, Noonan W, Nakane M, Brooks KA, Segreti JA, Polakowski JS, Cox B. Vitamin D receptor activation mitigates the impact of uremia on endothelial function in the 5/6 nephrectomized rats. *Int J Endocrinol*. 2010;2010:625852.
18. Zoccali C, Curatola G, Panuccio V, Tripepi R, Pizzini P, Versace M, Bolignano D, Cutrupi S, Politi R, Tripepi G, Ghiadoni L, Thadhani R, Mallamaci F. Paricalcitol and endothelial function in chronic kidney disease trial. *Hypertension*. 2014;64:1005–1011.
19. Lundwall K, Jörneskog G, Jacobson SH, Spaak J. Paricalcitol, microvascular and endothelial function in non-diabetic chronic kidney disease: a randomized trial. *Am J Nephrol*. 2015;42:265–273.
20. Lau WL, Leaf EM, Hu MC, Takeno MM, Kuro-o M, Moe OW, Giachelli CM. Vitamin D receptor agonists increase klotho and osteopontin while decreasing aortic calcification in mice with chronic kidney disease fed a high phosphate diet. *Kidney Int*. 2012;82:1261–1270.
21. Ritter CS, Zhang S, Delmez J, Finch JL, Slatopolsky E. Differential expression and regulation of klotho by paricalcitol in the kidney, parathyroid, and aorta of uremic rats. *Kidney Int*. 2015;87:1141–1152.
22. Kuro-o M, Matsumura Y, Aizawa H, Kawaguchi H, Suga T, Utsugi T, Ohyama Y, Kurabayashi M, Kaname T, Kume E, Iwasaki H, Iida A, Shiraki-Iida T, Nishikawa S, Nagai R, Nabeshima YI. Mutation of the mouse Klotho gene leads to a syndrome resembling ageing. *Nature*. 1997;390:45–51.
23. Nagai R, Saito Y, Ohyama Y, Aizawa H, Suga T, Nakamura T, Kurabayashi M, Kuroo M. Endothelial dysfunction in the Klotho mouse and downregulation of Klotho gene expression in various animal models of vascular and metabolic diseases. *Cell Mol Life Sci*. 2000;57:738–746.
24. Navarro-González JF, Donate-Correa J, Muros de Fuentes M, Pérez-Hernández H, Martínez-Sanz R, Mora-Fernández C. Reduced Klotho is associated with the presence and severity of coronary artery disease. *Heart*. 2014;100:34–40.
25. Stavenuiter AW, Arcidiacono MV, Ferrantelli E, Keuning ED, Vila Cuenca M, ter Wee PM, Beelen RH, Vervloet MG, Dusso AS. A novel rat model of vitamin D deficiency: safe and rapid induction of vitamin D and calcitriol deficiency without hyperparathyroidism. *Biomed Res Int*. 2015;2015:604275.
26. Barker SL, Pastor J, Carranza D, Quiñones H, Griffith C, Goetz R, Mohammadi M, Ye J, Zhang J, Hu MC, Kuro-o M, Moe OW, Sidhu SS. The demonstration of α Klotho deficiency in human chronic kidney disease with a novel synthetic antibody. *Nephrol Dial Transplant*. 2015;30:223–233.
27. Keese CR, Wegener J, Walker SR, Giaever I. Electrical wound-healing assay for cells in vitro. *Proc Natl Acad Sci U S A*. 2004;101:1554–1559.
28. R Foundation for Statistical Computing. R: a language and environment for statistical computing. 2017.
29. Vestweber D. VE-cadherin: the major endothelial adhesion molecule controlling cellular junctions and blood vessel formation. *Arterioscler Thromb Vasc Biol*. 2008;28:223–232.
30. Sakamoto T, Sakamoto H, Sheu SJ, Gabrielian K, Ryan SJ, Hinton DR. Intercellular gap formation induced by thrombin in confluent cultured bovine retinal pigment epithelial cells. *Invest Ophthalmol Vis Sci*. 1994;35:720–729.
31. Kusaba T, Okigaki M, Matui A, Murakami M, Ishikawa K, Kimura T, Sonomura K, Adachi Y, Shibuya M, Shirayama T, Tanda S, Hatta T, Sasaki S, Mori Y, Matsubara H. Klotho is associated with VEGF receptor-2 and the transient receptor potential canonical-1 Ca²⁺ channel to maintain endothelial integrity. *Proc Natl Acad Sci U S A*. 2010;107:19308–19313.
32. Chitalia N, Recio-Mayoral A, Kaski JC, Banerjee D. Vitamin D deficiency and endothelial dysfunction in non-dialysis chronic kidney disease patients. *Atherosclerosis*. 2012;220:265–268.
33. Stojanović M, Radenković M. Vitamin D versus placebo in improvement of endothelial dysfunction: a meta-analysis of randomized clinical trials. *Cardio-vasc Ther*. 2015;33:145–154.
34. Levin A, Tang M, Perry T, Zalunardo N, Beaulieu M, Dubland JA, Zerr K, Djurdjev O. Randomized controlled trial for the effect of vitamin D supplementation on vascular stiffness in CKD. *Clin J Am Soc Nephrol*. 2017;12:1447–1460.
35. Kumar V, Yadav AK, Lal A, Singhal M, Billot L, Gupta KL, Banerjee D, Jha V. A randomized trial of vitamin D supplementation on vascular function in CKD. *J Am Soc Nephrol*. 2017;28:3100–3108.
36. Won S, Sayeed I, Peterson BL, Wali B, Kahn JS, Stein DG. Vitamin D prevents hypoxia/reoxygenation-induced blood-brain barrier disruption via vitamin D receptor-mediated NF- κ B signaling pathways. *PLoS One*. 2015;10:e0122821.
37. Prasad N, Stevens T. The actin cytoskeleton in endothelial cell phenotypes. *Microvasc Res*. 2009;77:53–63.
38. Kong J, Zhang Z, Musch MW, Ning G, Sun J, Hart J, Bissonnette M, Li YC. Novel role of the vitamin D receptor in maintaining the integrity of the intestinal mucosal barrier. *Am J Physiol Gastrointest Liver Physiol*. 2008;294:G208–G216.
39. Tsujikawa H, Kurotaki Y, Fujimori T, Fukuda K, Nabeshima Y. Klotho, a gene related to a syndrome resembling human premature aging, functions in a negative regulatory circuit of vitamin D endocrine system. *Mol Endocrinol*. 2003;17:2393–2403.
40. Bloch L, Sineshcckova O, Reichenbach D, Reiss K, Saftig P, Kuro-o M, Kaether C. Klotho is a substrate for alpha-, beta- and gamma-secretase. *FEBS Lett*. 2009;583:3221–3224.
41. Kim HR, Nam BY, Kim DW, Kang MW, Han JH, Lee MJ, Shin DH, Doh FM, Koo HM, Ko KI, Kim CH, Oh HJ, Yoo TH, Kang SW, Han DS, Han SH. Circulating α -klotho levels in CKD and relationship to progression. *Am J Kidney Dis*. 2013;61:899–909.
42. Sakan H, Nakatani K, Asai O, Imura A, Tanaka T, Yoshimoto S, Iwamoto N, Kurumatani N, Iwano M, Nabeshima Y, Konishi N, Saito Y. Reduced renal α -Klotho expression in CKD patients and its effect on renal phosphate handling and vitamin D metabolism. *PLoS One*. 2014;9:e86301.
43. Koh N, Fujimori T, Nishiguchi S, Tamori A, Shiomi S, Nakatani T, Sugimura K, Kishimoto T, Kinoshita S, Kuroki T, Nabeshima Y. Severely reduced production of Klotho in human chronic renal failure kidney. *Biochem Biophys Res Commun*. 2001;280:1015–1020.
44. Rakugi H, Matsukawa N, Ishikawa K, Yang J, Imai M, Ikushima M, Maekawa Y, Kida I, Miyazaki J, Ogihara T. Anti-oxidative effect of Klotho on endothelial cells through camp activation. *Endocrine*. 2007;31:82–87.
45. Ikushima M, Rakugi H, Ishikawa K, Maekawa Y, Yamamoto K, Ohta J, Chihara Y, Kida I, Ogihara T. Anti-apoptotic and anti-senescence effects of Klotho on vascular endothelial cells. *Biochem Biophys Res Commun*. 2006;339:827–832.
46. Guan X, Nie L, He T, Yang K, Xiao T, Wang S, Huang Y, Zhang J, Wang J, Sharma K, Liu Y, Zhao J. Klotho suppresses renal tubulo-interstitial fibrosis by controlling basic fibroblast growth factor-2 signalling. *J Pathol*. 2014;234:560–572.
47. Yang K, Nie L, Huang Y, Zhang J, Xiao T, Guan X, Zhao J. Amelioration of uremic toxin indoxyl sulfate-induced endothelial cell dysfunction by Klotho protein. *Toxicol Lett*. 2012;215:77–83.

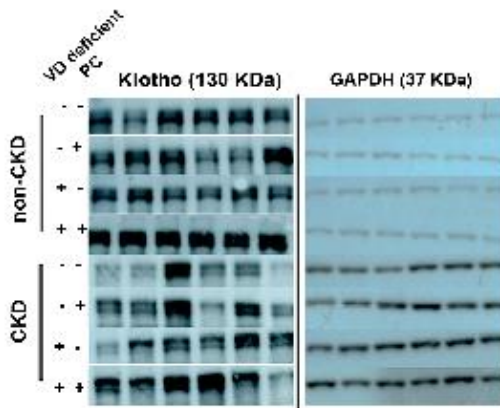
Supplemental Material

Figure S1. Kidney function and PTH serum levels in male Wistar rats (end-point).



Comparison of urea ($\mu\text{mol/l}$) (**A**) and creatinine (mmol/l) (**B**) serum measurements in CKD animals at week 11 ($n=7-8$). $p=0.0098$ for diet in creatinine. PTH (pg/ml) serum analysis at week 11 (**C**) (pooled groups $n=17-19$) and (**D**) (not pooled groups $n=4-5$). $p=0.003$ for surgery, $p=0.002$ for treatment, $p=0.007$ for diet and $p=0.024$ for treatment \times diet. Data are represented as means \pm SD. (non-CKD= non-uremic animals; CKD= uremic animals; VD= vitamin D; PC= paricalcitol). Differences were considered statistically significant for $p<0.05$ using unpaired t-test (C) two-way (A,B) and three-way ANOVA (D)** $p<0.01$.

Figure S2. α -Klotho protein in kidney tissue.



Representative Immunoblotting analysis of α -Klotho with KM2076 antibody in total protein lysates of Kidney (n=6-8). GAPDH was used as loading control. (non-CKD= non-uremic animals; CKD= uremic animals; VD= vitamin D; PC= paricalcitol).